Composition of a Neutron Star's Outer Crust

Author: Laiba Iqbal Kousar, liqbalko7@alumnes.ub.edu
Facultat de Física, Universitat de Barcelona, Diagonal 645, 08028 Barcelona, Spain.

Advisor: Xavier Roca Maza, xavier.roca.maza@fqa.ub.edu
(Dated: June 13, 2025)

Abstract: In the field of astrophysics, the study of neutron stars is often conducted to improve nuclear models. This work evaluates the composition of the outer crust of a cold non-accreting neutron star. The standard approach to the outer crust is considered: nuclei are fixed in a Coulomb lattice surrounded by a Fermi gas of free and degenerate electrons. It is shown that considering electrons as ultra-relativistic is a reasonably accurate approach for our purposes (99.98%). The nuclear composition of the lattice is studied by minimizing the Gibbs energy per baryon using a custom Python program. Additionally, the effect of the variations of the Liquid Drop Mass formula parameters on the crust composition is explored by: 1) calibrating the parameters to different experimental masses; and 2) systematically changing the asymmetry parameter.
Keywords: Stable nuclei, ultra-relativistic, binding energy parameters, Gibbs energy.
SDGs: This work is related to the UN Sustainable Development Goals 4, 7 and 9.

I. INTRODUCTION

The study of neutron stars (NS) plays a crucial role in the field of theoretical physics, as it bridges terrestrial physics with extreme conditions beyond experimental reach.

There are many types of neutron stars. They are characterized by age, size and other properties that are defined in the formation process of the star.

In a NS, each region (atmosphere, inner and outer crust, and inner and outer core) needs to be studied taking into account the different properties that govern them, thus different approximations can be applied. This study works with cold non-accreting NS at zero-temperature without magnetic field using the cold catalyzed matter hypothesis, which assumes that the star is in its most stable, lowest-energy configuration, at zero temperature and no external forces.

The subject matter of this work is the crust, which is often studied to improve nuclear models. It is defined as the region with completely ionized atomic nuclei. When compared to the nuclear saturation density ($\rho \sim 2,5 \cdot 10^{14}\ \mathrm{g\,cm^{-3}}$), the crust can be considered at low density. In this limit, the nuclei arrange in a lattice form. Throughout the study, it is assumed that at a given density there is only one species of nuclei in the lattice.

The nuclei lattice gets richer in neutrons as density increases, eventually leading to free neutrons forming a dense neutron gas [1]. While the outer crust has a free electron gas, the inner crust contains both free neutron and electron gas. The transition from atomically bound to unbound neutrons commences at the neutron drip line, when the Gibbs energy per particle reaches the neutron rest mass. At this point, β-decay processes produce unbound neutrons, releasing them in the electron gas, transitioning to the inner crust of the neutron star [2]. As pressure increases, the neutron gas gets more dense.

II. GIBBS ENERGY FOR A NEUTRON STAR

In order to study the ground state of a neutron star crust, one must minimize the energy. The Gibbs potential G is the most suitable as it ensures the continuity of pressure, thus thermodynamical equilibrium at all points.

$$G = U + PV - TS, \tag{1}$$

with U being the internal energy, P the pressure, V the volume, T the temperature and S the entropy.

The average temperature for a neutron star crust does not exceed $T \sim 10^9$K [6]. The thermal energy for the electron gas is proportional to the Boltzmann constant, therefore $k_{\mathrm{B}}T \sim$ KeV, and the temperature contribution can be considered negligible (because 1KeV $\ll$ 1MeV). In the following, it will be considered that T=0K.
The approximate range of values for baryon density in the outer crust is $n_{\mathrm{b}} \sim 10^4 - 4 \cdot 10^{11}\ \mathrm{g\,cm^{-3}}$ before the neutron drip takes place. Considering that $V \sim n^{-1}$, the Gibbs energy per nucleon can be rewritten as

$$\frac{G}{A} = g = \epsilon + \frac{P}{n_{\mathrm{b}}}, \tag{2}$$

where G is divided by the number of nucleons A, ϵ is the energy per baryon and n_{b} is the baryon density.

The microscopic structure of the crust is rather simple. At this density range, atoms are completely ionized. The atomic nuclei are fixed in a lattice structure, surrounded by a free degenerate electron gas. Although the specific structure is uncertain, many studies suggest that the most energetically stable structure is the BCC (*body-centered cubic*)[3]. Thus, the Gibbs energy per baryon can be written as a function of the energy per baryon and pressure of three independent terms: the nuclear (ϵ_{N}, P_{N}), electronic (ϵ_{e}, P_{e}) and lattice (ϵ_{l}, P_{l}) terms:

$$\epsilon = \epsilon_{\mathrm{N}} + \epsilon_{\mathrm{e}} + \epsilon_{\mathrm{l}}, \tag{3}$$

$$P = P_{\mathrm{N}} + P_{\mathrm{e}} + P_{\mathrm{l}}. \tag{4}$$

Each expression for the energy terms is defined by the system physics (sections II A, II B, II C), while the pressure can be found with the first thermodynamic principle for each contribution,

$$P_i = -\frac{\partial E_i}{\partial V} = {n_\mathrm{b}}^2 \frac{\partial \epsilon_i}{\partial n_\mathrm{b}}. \tag{5}$$

In this study, energy is expressed in MeV, n_i in fm^{-3}, and natural units, so $c = \hbar = 1$.

A. Nucleus

The energy contained in the nucleus is the rest mass in energy units minus the binding energy B, a strong-force interaction that maintains it together. Defining Z as the atomic number, A the atomic mass and $N = A - Z$:

$$\frac{E_\mathrm{N}}{A} = \epsilon_\mathrm{N} = m_\mathrm{n}\left(1 - \frac{Z}{A}\right) + m_\mathrm{p}\frac{Z}{A} - \frac{B(A,Z)}{A}, \tag{6}$$

where $m_\mathrm{p} = 938.272\mathrm{MeV}$, $m_\mathrm{n} = 939.557\mathrm{MeV}$, $m_\mathrm{e} = 0.511\mathrm{MeV}$. The first two terms are trivial, while the binding energy can be found using different nuclear models. Here, the liquid drop model is used [5]. The baryon density n_b is defined without distinguishing protons and neutrons. Since proton and neutron masses have a 1:1.0037 ratio, the baryon masses can be approximated as the neutron mass. Moreover, as neutron population grows when entering the crust, this approximation becomes more valid.

Since nuclei are considered point-like, their energy does not depend on $V \sim n^{-1}$, meaning the pressure contribution is zero, $P_\mathrm{N} = 0$.

1. *Weizsäcker formula*

Also known as the semi-empirical masses formula, the Weizsäcker formula gives an expression of the binding energy [5].

$$B(A,Z) = a_V A - a_S A^{2/3} + a_\mathrm{C}\frac{Z^2}{A^{1/3}} + a_\mathrm{A}\frac{(N-Z)^2}{A} + \frac{a_\mathrm{P}\delta}{A^{1/2}}, \tag{7}$$

The binding energy contains multiple elements, each scaled by a parameter, a_i, which depends on the contribution of each one. The first two terms correspond to the volumetric and surface contributions respectively. These two terms do not distinguish the nucleon type and only depend on the nucleon count. The third term refers to the Coulombic interactions between protons. The fourth is the asymmetry term due to the proton-neutron imbalance. In a NS with a known tendency to generate neutrons, the asymmetry term is important. The last term corresponds to the nucleon pairing energy, as a pair of like nucleons is more strongly bound than two unlike nucleons. The value of δ indicates whether the contribution of this term is positive, negative or zero depending on the pairing of protons and neutrons.

This is an empirical formula designed to adjust to empirical data, hence its name. Many studies have taken place to find the most accurate fit of the parameters iadjusting them to experimental data. These parameters often vary and have different applicability depending on restrictions considered for each fit. Generally, it shows better accuracy for heavy nuclei, as seen later in Fig.[2].

B. Electron gas

At NS crust densities and zero-temperature conditions, the electron gas behaves as a strongly degenerate and relativistic Fermi gas. Electrons will occupy the lowest energy states possible allowed by the Pauli exclusion principle, reaching the Fermi energy, the highest energy possible for an electron gas at zero-temperature. This way, the expression of the electronic energy contribution will be found with

$$\frac{E_\mathrm{e}}{A} = \epsilon_\mathrm{e} = \frac{1}{n_\mathrm{b}}\int_0^{p_{\mathrm{F,e}}} p^2\sqrt{p^2 + {m_\mathrm{e}}^4}\, dp. \tag{8}$$

In order to simplify algebra, the adimensional Fermi momentum and energy are defined as:

$$x_\mathrm{F} \equiv \frac{p_{\mathrm{F,e}}}{m_\mathrm{e}},\ y_\mathrm{F} = \sqrt{1 + {x_\mathrm{F}}^2},\ p_{\mathrm{F},i} \equiv (3\pi^2 n_i)^{1/3}. \tag{9}$$

After changing variables, integration gives the following expression, where the constant comes from treating it as an ideal, relativistic and degenerate gas of fermions.

$$\frac{E_\mathrm{e}}{A} = \epsilon_\mathrm{e} = \frac{{m_\mathrm{e}}^4}{8\pi^2 n_\mathrm{b}}[x_\mathrm{F} y_\mathrm{F}({x_\mathrm{F}}^2 + {y_\mathrm{F}}^2) - \ln(x_\mathrm{F} + y_\mathrm{F})]. \tag{10}$$

Using $n_\mathrm{e} = n_\mathrm{b}\left(\frac{Z}{A}\right)$ and Eq. (9), a dependence of ϵ_e on $p_{\mathrm{F,b}}(n_\mathrm{b}) \equiv p_\mathrm{F}$ is found, therefore electrons have a contribution to the pressure of the crust:

$$\begin{aligned} P_\mathrm{e} &= {n_\mathrm{b}}^2\frac{\partial \epsilon_\mathrm{e}}{\partial n_\mathrm{b}} = \frac{x_\mathrm{F}}{3}\frac{\partial(\epsilon_\mathrm{e} n_\mathrm{e})}{\partial x_\mathrm{F}} - \epsilon_\mathrm{e} n_\mathrm{e} \\ &= \frac{{m_\mathrm{e}}^4}{3\pi^2}\left[{x_\mathrm{F}}^3 y_\mathrm{F} - \frac{3}{8}[x_\mathrm{F} y_\mathrm{F}({x_\mathrm{F}}^2 + {y_\mathrm{F}}^2) - ln(x_\mathrm{F} + y_\mathrm{F})]\right]. \end{aligned} \tag{11}$$

1. *Ultra-relativistic approach*

In order to find an expression for the Fermi momentum p_F as a function of pressure, the expression $P(p_\mathrm{F})$ must be inverted. This is needed because energy and pressure expressions for electrons and the lattice depend on p_F, and P is the independent variable. However, Eq. (11) cannot be inverted analytically. Under the conditions of a NS, the electron gas can be considered as ultra-relativistic, so $p_{\mathrm{F,e}} \gg m_\mathrm{e}$ and $y_\mathrm{F} \approx x_\mathrm{F}$, This assumption simplifies the expression for P_e and makes it invertible,

$$\epsilon_{\mathrm{e,UR}} \approx \frac{{m_\mathrm{e}}^4}{8\pi^2 n_\mathrm{b}} 2{x_\mathrm{F}}^4, \qquad P_{\mathrm{e,UR}} \approx \frac{{m_\mathrm{e}}^4}{3\pi^2 n_\mathrm{b}}\frac{1}{4}{x_\mathrm{F}}^4. \tag{12}$$

C. Lattice

The energy contained in the lattice is due to Coulombic interaction. Since working in cartesian coordinates complicates the algebra, it is wiser to employ the Wigner-Seitz approximation [3]. Now, the lattice is considered to be formed by spheres of radius r_0, so that the volume is the same as that of the unitary cell of a BCC. This sphere contains one ion at the center and an electron gas around it. The three Coulombic interactions that constitute the energy of a unitary cell are: ion-ion, electron-ion and electron-electron.

$$E_{\text{cell}} = E_{\text{i-i}} + E_{\text{e-i}} + E_{\text{e-e}}. \tag{13}$$

With only one nucleus at the center, there is no ion-ion interaction. The other two terms can be easily found using the Coulombic interaction theory of a nucleus with Z protons and Z electrons.

$$\begin{aligned} E_{\{\text{cell}} &= \int^{r_0} \frac{Ze}{r} dq(r) + \int^{r_0} \frac{q(r)}{r} dq(r) \\ &= \frac{-3}{2}\frac{Z^2e^2}{r_0} + \frac{3}{5}\frac{Z^2e^2}{r_0}. \end{aligned} \tag{14}$$

The dependence on r_0 can be derived into a dependence on n_{b} using the volume definition of the sphere and the unitary cell of a BCC, and then can be expressed in terms of p_{F} using Eq. (9). To retrieve back the BCC structure from the Wigner Seitz approximation, the 9/10 factor is replaced by 0.89593 [1].

$$\frac{E_{\text{cell}}}{A} = \epsilon_{\text{l}} = \frac{-9}{10}\frac{Z^2e^2}{Ar_0} = -C_{\text{l}}\frac{Z^2}{A^{4/3}}p_{\text{F}}, \tag{15}$$

where $C_{\text{l}} = 3.40665 \cdot 10^{-3}$. Now the expression for the lattice pressure can be easily found:

$$P_{\text{l}} = n_{\text{b}}^2 \frac{\partial \epsilon_{\text{l}}}{\partial n_{\text{b}}} = -Cl\frac{n_{\text{b}}}{3}\frac{Z^2}{A^{4/3}}p_{\text{F}}. \tag{16}$$

D. Final Gibbs expression

The final expression for the Gibbs energy can be rewritten doing another change of variables to simplify it. The new variables are defined as $x \equiv A^{1/3}$ and $y \equiv Z/A$. With this, $p_{\text{F,e}} = p_{\text{F}}y^{1/3}$, and it is finally obtained that:

$$\begin{aligned} \frac{B(x,y)}{A} &= a_V - \frac{a_s}{x} + a_{\text{C}}(x^2y^2) + a_{\text{A}}(1-y^2) + \frac{a_{\text{P}}\delta}{x^{3/2}}, \\ \epsilon_{\text{N}} &= ym_{\text{p}} + (1-y)m_{\text{n}} - \frac{B(x,y)}{A}, \end{aligned} \tag{17}$$

and the thermodynamic variables are

$$\epsilon(x,y,p_{\text{F}}) = \epsilon_{\text{N}} + \frac{3}{4}y^{4/3}p_{\text{F}} - C_{\text{l}}x^2y^2p_{\text{F}}, \tag{18}$$

$$P(x,y,p_{\text{F}}) = \frac{n_{\text{b}}}{4}y^{4/3}p_{\text{F}} - \frac{n_{\text{b}}}{3}C_{\text{l}}x^2y^2p_{\text{F}}, \tag{19}$$

$$g(x,y,p_{\text{F}}) = \epsilon_{\text{N}} + y^{4/3}p_{\text{F}} - C_{\text{l}}\frac{4}{3}x^2y^2p_{\text{F}}. \tag{20}$$

III. RESULTS

A. UR approximation

Considering the electron gas of a NS as ultra-relativistic may help with the algebra, but is it accurate? This approximation can be verified comparing how much P changes with and without UR approximation.

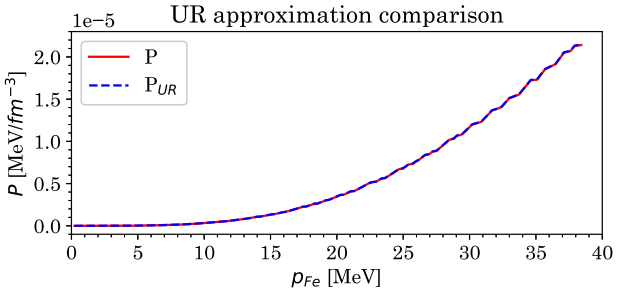

FIG. 1: Comparison of pressure with and without UR approximation.

Fig. [1] shows that the difference between Eqs. (11) and (12) is negligible. The accuracy of the UR approximation is about 99.98%. Finding the values for p_{F} without this approximation is possible, but complicates the computation process and gives room for more errors during the minimization of the Gibbs energy. Once the UR approximation is verified, $P_{\text{e,UR}}$ can be used to minimize the Gibbs energy and find the stable nuclei in the crust.

B. NS outer crust composition

Minimizing Eq.(20) involves finding x and y that give its lowest value for a given pressure. Pressure is implicit in the $p_{\text{F}}(P)$ expression that comes from inverting Eq. (19). The first step is to find the parameters of the binding energy.

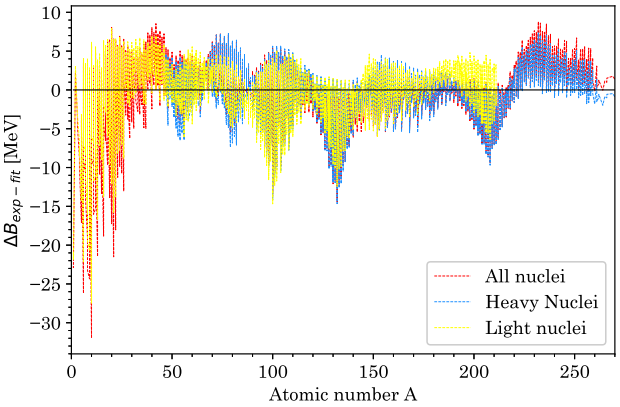

FIG. 2: Difference between experimental data of the binding energy and Eq. (7) for different ranges of data: all data, light nuclei and heavy nuclei.

Fig. [2] shows the difference between experimental data and Eq. (7) for each atomic number. Values for lighter nuclei fluctuate considerably, meaning that the

Weizsäcker formula works better for heavy nuclei. This is because the formula is based on the liquid drop model, and light nuclei do not resemble a spherical drop as much. Additionally, since neutron stars are expected to have heavier nuclei (Fe and above), the fit used will be that of heavy nuclei. The parameters used to minimize the Gibbs energy are: $a_V = (15.49 \pm 0.03)$MeV, $a_S = (16.74 \pm 0.10)$MeV, $a_C = (0.700 \pm 0.002)$MeV, $a_A = (22.77 \pm 0.09)$MeV, $a_P = (0.46 \pm 0.03)$MeV.

For a baryon density range $n_b \sim 10^4 - 10^{11}\,\mathrm{g\,cm^{-3}}$, Table. [I] shows the stable nuclei that minimize the Gibbs energy found with a custom Python algorithm, reaching neutron drip with ^{154}Cd.

P(MeV fm^{-3})	n (g cm^{-3})	Z	N	Element
$1.00{\cdot}10^{-12}$	$8.71{\cdot}10^{4}$	26	31	^{57}Fe
$1.04{\cdot}10^{-9}$	$1.63{\cdot}10^{7}$	26	32	^{58}Fe
$9.73{\cdot}10^{-8}$	$5.01{\cdot}10^{8}$	28	36	^{62}Ni
$1.84{\cdot}10^{-6}$	$4.78{\cdot}10^{9}$	30	42	^{72}Zn
$1.27{\cdot}10^{-5}$	$2.16{\cdot}10^{10}$	32	49	^{81}Ge
$4.44{\cdot}10^{-5}$	$5.81{\cdot}10^{10}$	36	60	^{96}Kr
$1.71{\cdot}10^{-4}$	$1.76{\cdot}10^{11}$	40	77	^{117}Zr
$2.97{\cdot}10^{-4}$	$2.82{\cdot}10^{11}$	44	92	^{138}Ru
$3.79{\cdot}10^{-4}$	$3.45{\cdot}10^{11}$	46	99	^{145}Pd
$4.35{\cdot}10^{-4}$	$3.91{\cdot}10^{11}$	48	106	^{152}Cd
$4.67{\cdot}10^{-4}$	$4.17{\cdot}10^{11}$	48	108	^{154}Cd

TABLE I: Stable nuclei for different values of pressure. For densities closer to the drip line, the number of neutrons grows faster, suggesting neutron richness near the inner crust.

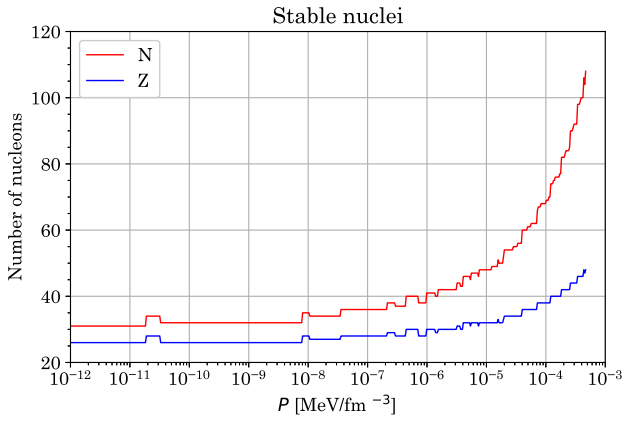

FIG. 3: Number of protons and neutrons that minimize the Gibbs energy. Nuclei get heavier and become neutron-rich for higher pressure.

Fig. [3] shows the number of protons and neutrons that minimize the Gibbs energy for a given pressure. For lower pressures, the stable nuclei are near ^{57}Fe, but as pressure rises, nuclei tend to get heavier and richer in neutrons, reaching the neutron drip point with ^{154}Cd.

C. Parameter variation

Most of the terms used in the Gibbs energy are found through theoretical deductions, which makes it hard to vary them to get different results and study from a different perspective. However, some terms are based on computational calculations, like the precise contribution of the BCC lattice or the parameters of $B(x, y)$. Although the lattice approximation is hard to specify more accurately without a thorough calculation (and has a small contribution to the Gibbs energy, therefore would not make a big difference), changing the parameters for the binding energy is a more tangible study and could lead to interesting results.

Fig. [3] uses the parameters fitting for heavy nuclei. The same can be done using all nuclei or just light nuclei. As result, for changes in just one term of the total Gibbs energy (Eq. (20)), the stable nuclei evolution changes considerably, as later seen in Table [II]. This raises the question of which parameters of $B(x, y; P)$ affect most in the minimization of the Gibbs energy for a NS.

Proton fraction ($y = Z/A$) reduces when pressure rises (see Fig. [A5]), meaning that the difference between protons and neutrons becomes larger with pressure. While other terms may not directly take this into account, the asymmetry term, $a_A \frac{(N-Z)^2}{A}$, affects the contribution of proton fraction in the Gibbs energy. Therefore, studying how the asymmetry parameter can alter the stable nuclei will possibly take an impact on neutron richness.

D. Asymmetry parameter

To analyze different for values of a_A, it is held constant, and the experimental data is used to fit the remaining parameters. While doing so, the fit should maintain enough accuracy to properly describe nuclei, therefore should not deviate too much from the parameters obtained by fitting all 5 parameters to the dataset.

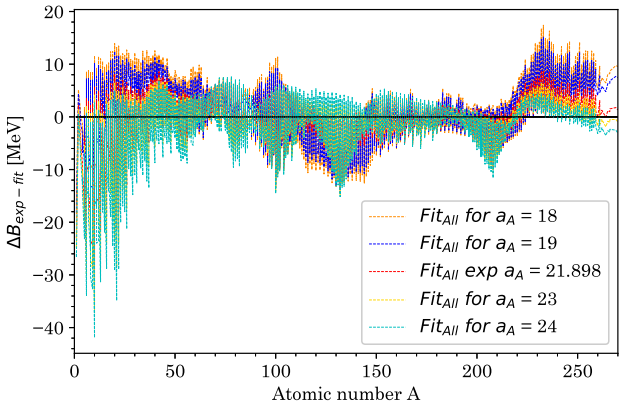

FIG. 4: A comparison for the different fits and their adjustment to all experimental data.

Fig. [4] shows the fitting of the parameters of $B(x, y; P)$ using all nuclei data, fixing the value of a_{A}. The parameters that fit best correspond to $a_{\mathrm{A}} = 23\mathrm{MeV}$, and are closer to the parameters obtained by fitting for heavy nuclei. This was found by comparing the variance of B for each parameter evaluation (See Table. [AIII]).

This emphasizes that the Weizsäcker formula works better for heavier nuclei. This result also suggests that the semi-empirical mass formula (Eq. (7)) may have a more accurate expression, since the parameters that fit all the data the best are not the ones found by doing a direct fitting.

Once the stable nuclei for these fixed parameters are calculated, they can be compared to see how much neutron-richness is affected at the drip line, see the next Table for the nuclei at the outer layer of the crust and at the drip line.

Fit	a_{A} (MeV)	Initial element (n=8.65·10^4)	n_{Drip} ($10^{11}\mathrm{gcm}^{-3}$)	Drip element
All	18	^{48}Ti	5.86	^{190}Sn
All	19	^{48}Ti	5.33	^{182}Sn
All	23	^{55}Mn	4.56	^{162}Cd
All	24	^{57}Fe	4.12	^{151}Ag
All	21.89	^{55}Mn	4.34	^{158}Cd
Large A	22.82	^{57}Fe	4.17	^{156}Cd
Small A	20.81	^{57}Fe	4.62	^{164}Sb

TABLE II: Values of the stable nuclei for initial density and the neutron drip one, also the value of the density when the neutron drip is reached can vary. These values are found using all nuclei data.

Table. (II) contains the nuclei obtained for the lowest pressure considered, and the nuclei obtained at the neutron drip line. Smaller values for a_{A} are related to fitting for lighter nuclei and give very neutron rich nuclei near the drip line and higher drip pressure, but the fit of these parameters describes $B(x, y; n_{\mathrm{b}})$ with less accuracy. Fitting for heavier nuclei results in a higher value for a_{A}, but if exceeded too much, it also starts to show inaccuracy. For these parameters, the neutron drip line is achieved with smaller nuclei and less pressure.
Table. (AIII) shows the deviations of each fit.

IV. CONCLUSIONS

This article investigates the stable nuclei present in a neutron star crust using recent binding energy measurements [8]. The evolution of these nuclei stops when the neutron drip line is reached. First, the ultra-relativistic approximation is validated, proving that it simplifies expressions while maintaining a 99.98% accuracy.

Then, the evolution of stable nuclei was mapped starting at ^{57}Fe for the outer crust, and finishing with ^{154}Cd at the drip line with $n_{\mathrm{b}} = 4.17 \cdot 10^{11}\mathrm{g\,cm}^{-3}$. Beyond this point, the inner crust begins, where neutron drip continues until $n_{\mathrm{b}} \sim 2.5 \cdot 10^{14}\mathrm{g\,cm}^{-3}$ [1].

Lastly, the impact of the binding energy fit on the results for stable nuclei is analyzed using two different approaches:

i. adjusting the data range for the fitting of the binding energy: we find that different ranges give different parameters that have an impact on the values of the stable nuclei, lighter nuclei give more neutron-rich nuclei at the drip line, but fit the binding energy worse than heavy nuclei,

ii. fixing the asymmetry parameter: for values near parameter a_{A} derived from the experimental data, the impact of the variation of the proton-neutron asymmetry term in the finding of stable nuclei in the crust is analyzed. Obtaining different nuclei from the initial parameters is possible but it rapidly compromises the accuracy of the fit.

Acknowledgments

I would like to express my deepest gratitude to my advisor Xavier Roca Maza for advising me through the development of this study and guiding me every step of the way with inexhaustible patience. I would also like to thank my peers for their encouragement and motivation, as well as my family for supporting and accommodating me while I was working on this TFG.

[1] Chamel, N. & Haensel, P. (2008). Physics of Neutron Star Crusts, *Living Rev. Relativity, 11, 10.*
[2] Alford, M., & Harris, S. (2018). β equilibrium in neutron-star mergers.*Physical Review C*, 98(6).
[3] Haensel, P., Potekhin, A. Y. & Yakovlev, D. G. (2006). *Neutron Stars 1: Equation of State and Structure.* Springer.
[4] Chamel, N. (2008). *Neutron star crust beyond the Wigner-Seitz approximation, in Exotic States of Nuclear Matter.*
[5] Williams, W. S. C. (1991). *Nuclear and Particle Physics.*
[6] Haensel, P. (2001). Neutron Star Crusts. In: Blaschke, D., Sedrakian, A., Glendenning, N.K. (eds) *Physics of Neutron Star Interiors. Lecture Notes in Physics*, vol 578.
[7] Roca-Maza, X. & Piekarewicz, J. (2018). Impact of the symmetry energy on the outer crust of non-accreting neutron stars. *Physical Review C,* 78(2).
[8] Huang, W. J., Meng, W., Kondev, F. G., Audi, G. & Naimi, S. (2021). *The AME 2020 atomic mass evaluation (I) & (II)*

Estudi de la crosta externa d'una estrella de neutrons

Author: Laiba Iqbal Kousar, liqbalko7@alumnes.ub.edu
Facultat de Física, Universitat de Barcelona, Diagonal 645, 08028 Barcelona, Spain.

Advisor: Xavier Roca Maza, xavier.roca.maza@fqa.ub.edu
(Dated: June 13, 2025)

Resum: En el camp de l'astrofísica, l'estudi de les estrelles de neutrons sovint es realitza per millorar els models nuclears. Aquest treball avalua la composició de l'escorça exterior d'una estrella de neutrons freda i sense acreció. Es considera l'aproximació estàndard a l'escorça externa: els nuclis estan fixats en una xarxa de Coulomb envoltada per un gas de Fermi d'electrons lliures i degenerats. Es demostra que considerar els electrons com a ultra-relativistes és un enfocament raonablement precís per als nostres propòsits (99,98%). La composició nuclear de la xarxa s'estudia minimitzant l'energia de Gibbs per barió utilitzant un programa Python personalitzat. A més, s'explora l'efecte de les variacions dels paràmetres de la fórmula del model de gota líquida a la composició de l'escorça mitjançant: 1) calibratge dels paràmetres a diferents masses experimentals; i 2) canvi sistemàtic del paràmetre d'asimetria.
Paraules clau: Nuclis estables, ultrarrelativistic, parametres, energia de lligam, energia de Gibbs.
ODSs: Aquest TFG està relacionat amb els Objectius de Sostenibilitat 4, 7 i 9 de les Nacions Unides.

Objectius de Desenvolupament Sostenible (ODSs o SDGs)

1. Fi de la es desigualtats		10. Reducció de les desigualtats	
2. Fam zero		11. Ciutats i comunitats sostenibles	
3. Salut i benestar		12. Consum i producció responsables	
4. Educació de qualitat	X	13. Acció climàtica	
5. Igualtat de gènere		14. Vida submarina	
6. Aigua neta i sanejament		15. Vida terrestre	
7. Energia neta i sostenible	X	16. Pau, justícia i institucions sòlides	
8. Treball digne i creixement econòmic		17. Aliança pels objectius	
9. Indústria, innovació, infraestructures	X		

Aquest treball es relaciona amb els ODS 4 (Educació de qualitat) concretament amb les fites 4.3 i 4.c perquè promou l'educació en l'àmbit universitari i promou la formació de docents formats en l'àmbit del treball. També es vincula amb l'ODS 7 (Energia neta i assequible), a la fita 7.a perquè facilita i promou l'accés a informació rellevant per poder avançar en l'eficiència energètica. Finalment, es relaciona amb l'ODS 9 (Indústria, innovació, infraestructures), fites 9.4 i 9.5 per fer aportacions que permetran utilitzar recursos nuclears amb major eficàcia i fomentar en la innovació i desenvolupament científics al seu voltant.

GRAPHICAL ABSTRACT

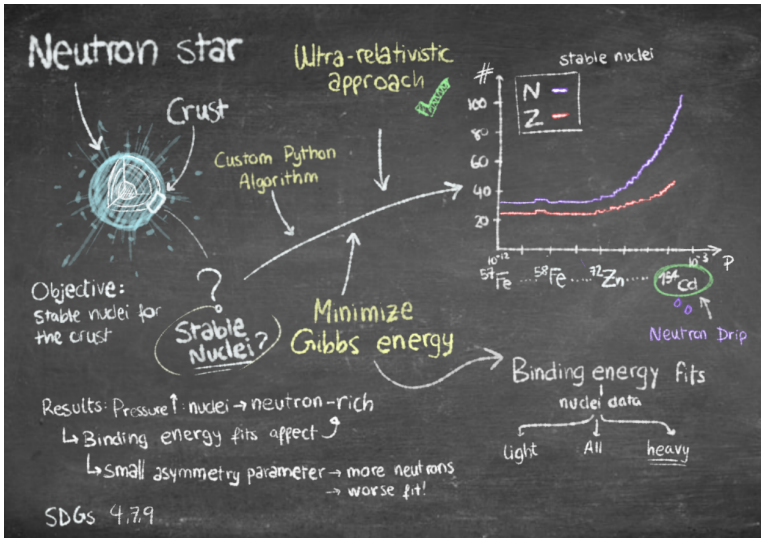

Appendix A: SUPPLEMENTARY MATERIAL

This appendix contains figures regarding the article that may be useful to understand some results.

1. Proton fraction

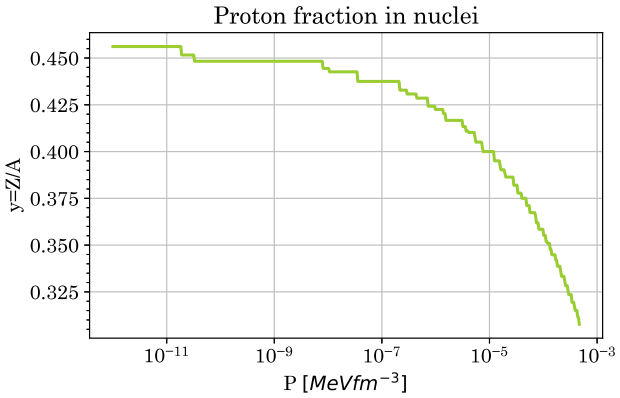

FIG. 5: Evolution of the proton fraction with rising pressure in the crust. The pressure axis is in logarithmic scale.

Fig. (5) shows the evolution of the proton fraction for the heavy nuclei fit. As pressure increases, the proportion of protons within the nuclei decreases. Initially, the proton fraction is slightly above 0.45, and gradually decreases to almost 0.30. This shows a tendency of nuclei to get rich in neutrons. With the increase of pressure, the neutron enrichment rate accelerates.

2. Parameter fitting

Fit	a_A (MeV)	$\langle \Delta B_{exp-fit} \rangle$ (MeV)	σ_B
Large A	18	3.991	3.286
Large A	19	3.438	2.850
Large A	21.898	2.314	2.047
Large A	23	2.263	2.020
Large A	24	2.482	2.110
All	18	4.510	3.538
All	19	3.850	3.074
All	21.898	2.608	2.619
All	23	2.586	2.917
All	24	2.861	3.325
All	21.898	2.608	2.619
Large A	22.767	2.245	1.993
Small A	20.808	2.380	2.250

TABLE III: Values of the different fits considered in the article, with their respective mean values and standard deviation σ_B. The mean values and and σ_B are calculated with the absolute value of the difference between the experimental data and the fit.

To determine the most accurate fit, several factors were considered. To begin, for each fixed a_A value, two fitting approaches were done, one with all the data, and one with large nuclei data (Fe and above). The third column presents the mean deviation between experimental and fitted binding energy values. A small value of the mean deviation is an indicative of a better fit. The fourth column is the standard deviation of $\Delta B_{exp-fit}$ further checking accuracy.

The same analysis was done to the 5-parameter fitting in the three cases: using all data, light nuclei and heavy nuclei data. For the case of the asymmetry parameter study, the fit with $a_A = 23$MeV shows the smaller deviations for most calculations, except the standard deviation for all nuclei with this parameter. The mean deviation is still smaller than that for the other values. Similarly, when fitting for different data set ranges, $a_A = 22.767$MeV (corresponding to heavy nuclei) presents the smallest deviations in respect to the other fits.

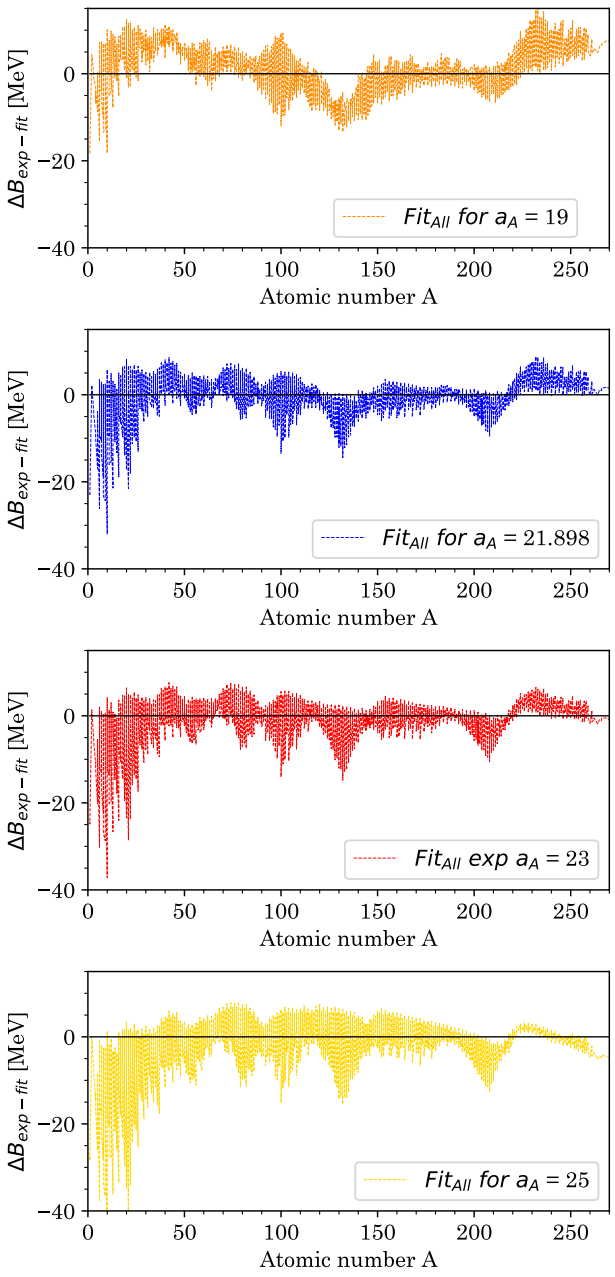

FIG. 6: Binding energy fit using different values for the fixed parameter, a_{A}, plotted separately to compare the differences between each fit.

Fig. (7) shows how the evolution of the stable nuclei in the crust varies depending on the dataset used to fit the parameters. This happens because the dataset choice affects the values of the parameters, which has a high impact on the Gibbs energy. All three cases show a tendency to get neutron rich with increasing pressure, but for the light nuclei fit, there is a noticeable increment of the neutron population for pressures near the neutron drip line.

Fig.(6) shows the variation of the fit accuracy when using different values for the asymmetry parameter, representing all the dataset. For $a_{\mathrm{A}} = 21.898, 23\mathrm{MeV}$, the fit has the lowest error values. When the parameter is below these values, although the stable nuclei for the neutron star crust get significantly neutron-rich (Table. II), the fit fails to describe the binding energy, therefore any result obtained with these parameters would not be realistic. The same happens with values that are much higher, the fit shows bigger deviations and wider discrepancies with the experimental data.

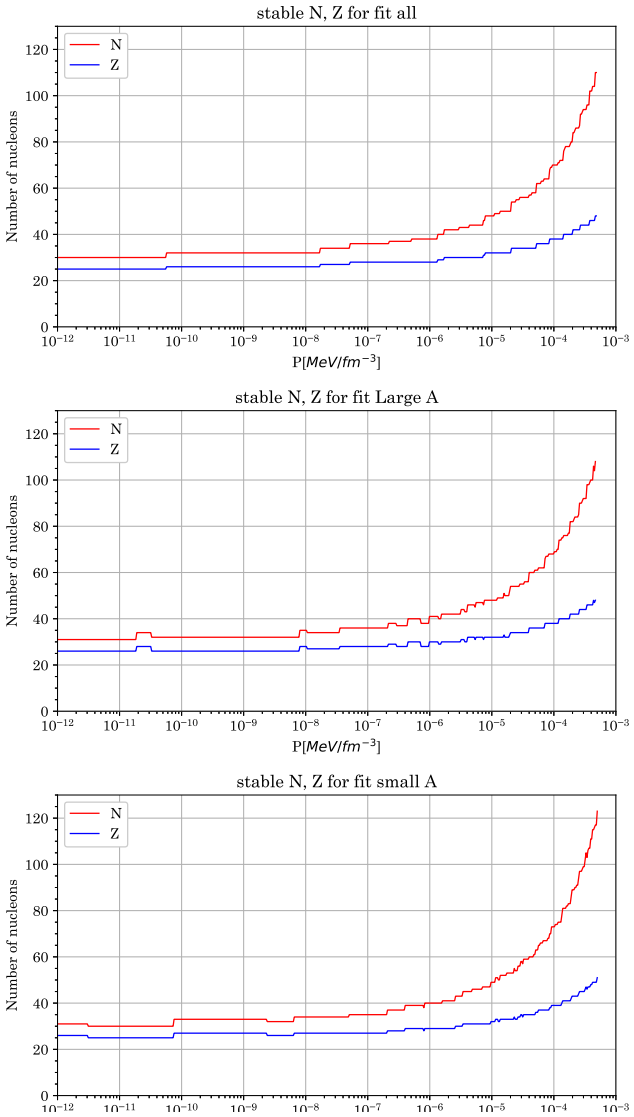

FIG. 7: Comparison of the nuclei that minimize de Gibbs energy for each data fit considered. The heavier the nuclei considered for the fitting of the parameters reach the drip line earlier, while fitting for lighter nuclei allows to have more neutron-richness in the atomic structure before reaching the drip line.